iScience

CellPress
OPEN ACCESS

Article

High-throughput submicron-resolution microscopy of *Caenorhabditis elegans* populations under strong immobilization by cooling cultivation plates

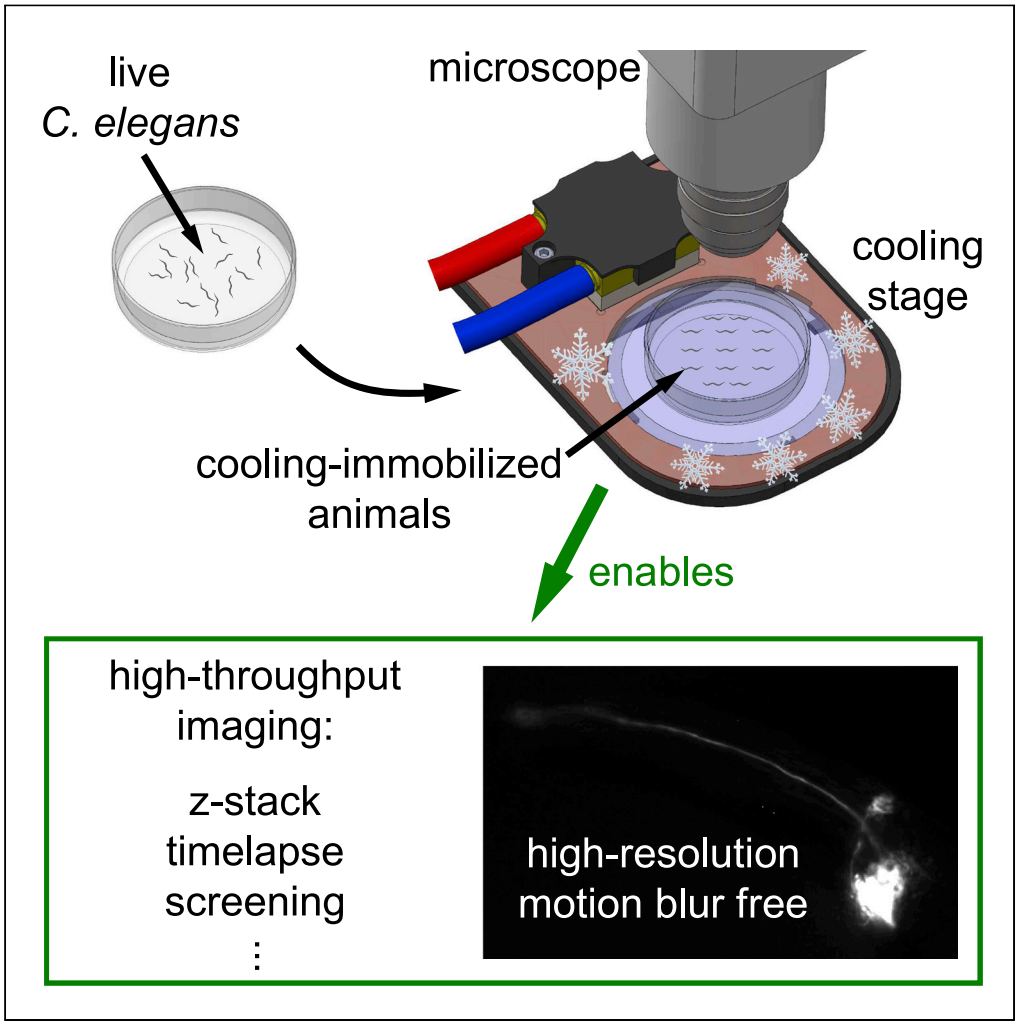

Yao L. Wang, Noa W.F. Grooms, Erik L. Jaklitsch, Leilani G. Schulting, Samuel H. Chung

schung@northeastern.edu

Highlights

Relatively warmer temperatures more strongly immobilize animals

Cooling enables high-resolution fluorescence imaging free from motion blur

Cooling approach reduces animal processing time for imaging by >98%

Rapid imaging permits high-throughput experiments for biological discovery

Wang et al., iScience 26, 105999
February 17, 2023
https://doi.org/10.1016/j.isci.2023.105999

iScience

CellPress
OPEN ACCESS

Article

High-throughput submicron-resolution microscopy of *Caenorhabditis elegans* populations under strong immobilization by cooling cultivation plates

Yao L. Wang,[1,2] Noa W.F. Grooms,[1,2] Erik L. Jaklitsch,[1,2] Leilani G. Schulting,[1] and Samuel H. Chung[1,3,*]

SUMMARY

Despite its profound impact on biology, high-resolution *in vivo* microscopy largely remains low throughput because current immobilization techniques require substantial manual effort. We implement a simple cooling approach to immobilize entire populations of the nematode *Caenorhabditis elegans* directly on their cultivation plates. Counterintuitively, warmer temperatures immobilize animals much more effectively than the colder temperatures of prior studies and enable clear submicron-resolution fluorescence imaging, which is challenging under most immobilization techniques. We demonstrate 64× z-stack and time-lapse imaging of neurons in adults and embryos without motion blur. Compared to standard azide immobilization, cooling immobilization reduces the animal preparation and recovery time by >98%, significantly increasing experimental speed. High-throughput imaging of a fluorescent proxy in cooled animals and direct laser axotomy indicate that the transcription factor CREB underlies lesion conditioning. By obviating individual animal manipulation, our approach could empower automated imaging of large populations within standard experimental setups and workflows.

INTRODUCTION

The nematode *Caenorhabditis elegans* is a widely utilized model organism for studying many biological processes. Similar to microorganisms, *C. elegans* are typically cultivated on agarose plates, and they reproduce rapidly by self-fertilization, making them well suited for studies that require a large sample size. Their transparency and a wide array of labeling techniques allow straightforward visualization of their internal anatomy. Many studies in *C. elegans* image subcellular structures at submicron resolution, which necessitates animal immobilization to prevent image blur. Proper immobilization is especially crucial for techniques involving multiple images in space or time, such as 3D image stacks (*i.e.*, z-stacks) and time-lapse imaging. Typically, immobilization involves manual manipulation of individual animals and mounting them on slides. These time- and labor-intensive procedures restrict experiments to small sample sizes.

Many strategies have been developed to immobilize *C. elegans*, but there are distinct drawbacks for each (see Table S1). In brief, chemical methods utilize agents such as sodium azide or levamisole to immobilize by disrupting animal physiology.[1] Mechanical methods, such as polystyrene beads and hydrogel mixtures, physically restrain animals by pressure, viscosity, or friction.[2] Microfluidic and on-chip technologies constrain animals by pressure, compression, or suction against a membrane or fluid.[3,4] Lastly, extreme temperatures can also immobilize animals, and most techniques cool animals in flooded wells or microfluidics.[5] Even with these advanced immobilization strategies, several significant drawbacks remain: Some of the above strategies require fabrication of slides and significant manual pre- and postprocessing of individual animals. They may increase physiological or physical stress on animals.[6] Some strategies require complex fabrication and setups or require significant user training. Several methods may also allow small animal movements that blur images, particularly in the nose and pharynx. Notably, none of the current strategies allow for direct imaging on cultivation plates, necessitating time-consuming animal transfer.

Here, we address these shortcomings by developing an approach that readily and reversibly immobilizes entire animal populations with minimal user effort. We describe a thermoelectric cooling stage and

[1]Department of Bioengineering, Northeastern University, Boston, MA 02115, USA

[2]These authors contributed equally

[3]Lead contact

*Correspondence: schung@northeastern.edu

https://doi.org/10.1016/j.isci.2023.105999

associated methods that can immobilize *C. elegans* en masse directly on cultivation plates for high-resolution imaging. Our cooling instrument (which we named *Copli*: cold plate immobilization) stably holds the entire cultivation plate at a desired temperature. We characterize animal movement at several target temperatures and under different cooling rates. Surprisingly, for animals cultivated at 20°C, we found that cooling to relatively higher temperatures, specifically 6°C, minimizes animal movement, though previously reported cooling strategies utilized temperatures between 2°C and 4°C.[5,7] Animal movement while cooled consists of bouts of submicron nose tip movement occurring infrequently enough to permit high-resolution bright-field imaging during timescales on the order of minutes. Cooling for an hour does not impact *C. elegans* fecundity or lifespan. Using our novel immobilization method, we obtain submicron-resolution wide-field microscope z-stacks and time-lapse images of fluorescent neurons in *C. elegans* adults and embryos without blurring from animal motion. We demonstrate that our approach eliminates the need for most of the animal processing steps and greatly accelerates the pace of high-resolution imaging in *C. elegans*. We also show that the cooling stage enables large-scale imaging that would otherwise be time-prohibitive with conventional animal processing and imaging. We envision that cooling immobilization could form the basis for automated imaging of large *C. elegans* populations on common experimental setups and workflows.

RESULTS

Cooling stage apparatus and temperature distribution

Our instrument design goal is to uniformly cool an entire 55-mm diameter agar cultivation plate to a target temperature, immobilizing animals for high-resolution fluorescence imaging while also preserving transillumination and access to animals. Agar plates are commonly used for cultivating, observing, and manipulating *C. elegans*, so our instrument has broad applicability. As shown in Figures 1A and 1B, the Copli instrument comprises a thin stage made of an 80-mm diameter transparent sapphire window, a highly conductive copper body, a thermoelectric Peltier heat pump, and a closed-loop liquid cooler. The sapphire window is transparent for transillumination and has a high thermal conductivity. We designed notch cutouts next to the colder side of the sapphire window to improve temperature uniformity across the window. The Peltier is a thermoelectric, solid-state device that pumps heat between its two sides depending on applied voltage.

The stage rapidly cools agar plates resting on the sapphire window. Heat leaves the plate to the sapphire window and then transfers to the copper body and Peltier. The Peltier pumps heat to the closed-loop cooler for removal. Thermal simulation of our design predicted a uniform thermal distribution (<1°C temperature difference from target temperature, T_{set}) across the central 40-mm diameter area of the cultivation plate (Figure 1B thermal simulation top view). We constructed, assembled, and preliminarily tested the device by achieving and holding a variety of temperatures on the agar surface (Figure 1C) while the device is situated on an upright microscope stage. We measured the thermal distribution of the agar plate and cooling stage, demonstrating an even distribution across the plate's central area and ensuring that the animals are held at the same temperature for uniform immobilization (Figure 1D). Thus, Copli's features include optical transparency for transillumination, high thermal conductivity for cooling efficiency, and uniform temperature distribution across the agar surface.

General observations of cooling immobilization on agarose plates

Because our study is the first, to our knowledge, to immobilize animals on agar plates by cooling, we began by carefully characterizing the impact of temperature on movement of animals cultivated at 20°C and 15°C. Most animals are not immobilized by temperatures ≥8°C and crawl out of the imaging field of view within minutes. Similar to prior studies of animals in liquid solution, cooling to 1°C–7°C slows *C. elegans* movement and stops crawling on plates immediately. Under cooling immobilization, the nose of the animal moves the most of any body part. Pharyngeal pumping is strongly suppressed, the tail also shows some movement, and the body moves the least. Video S1 shows typical examples of immobilized animal movement on a cultivation plate at 6°C. The frame rate is sped up 50× to show a 1200-s time span in a short video. The body parts are immobilized to slightly different levels, consistent with the independent control of these parts[8] and our experience with sodium azide anesthesia.[9] Because the nose tip exhibits the most movement and contains our target neuron, we verify our cooling immobilization by measuring movement of the nose tip throughout our work described below.

Optimal cooling temperature for immobilization

We next determined the optimal target temperature, T_{set}, to immobilize animals. The standard cultivation temperature (T_{cult}) for *C. elegans* is 20°C, and we utilized it for all experiments, except characterizing immobilization of 15°C-cultivated animals. Previous reports utilized target temperatures of 2°C–4°C[5,7] but

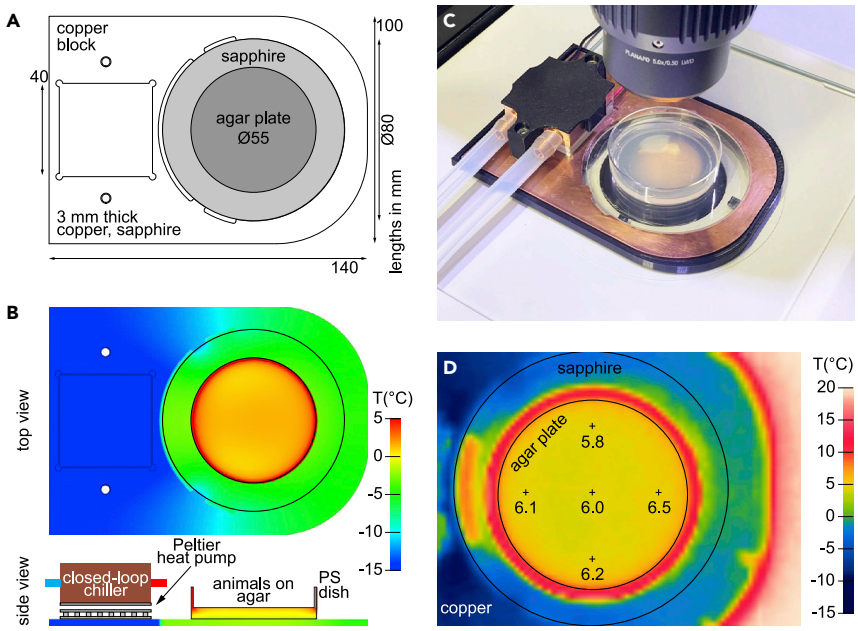

Figure 1. Cooling stage apparatus

(A) Top-down view of cooling immobilization stage. Agar cultivation plates placed on the sapphire window.

(B) Thermal modeling of stage and agar plate. Peltier heat pump and liquid cooling system secured to the copper base.

(C) Photograph of cooling stage and agar plate on upright microscope.

(D) Thermal image of unlidded agar plate and stage cooled to T_{set} = 6°C obtained by infrared camera. Temperatures at indicated points.

presented minimal quantitative or qualitative characterization of movement. In our experience, some animal movement, however slow or small, persists at all physiologically relevant temperatures. We have even observed movement of animals in supercooled buffer held well below 0°C. By cooling plates to 1°C–7°C using our instrument, we quantitatively investigated animal immobilization in response to a wide temperature range. Surprisingly, we found that a relatively higher temperature, 6°C, is the optimal temperature for immobilization of animals raised at 20°C. Figure 2 shows average nose tip velocity for each minute at specified times after reaching T_{set}. At 1°C–3°C, nose movement velocity is slow initially but does not greatly decrease over the hour after reaching T_{set} (Figure 2A). We confirmed that this persistent velocity trend continued for at least 2 h after reaching T_{set} (see below for details). At these velocities (0.5–1.0 μm/s), we could not obtain clear high-resolution z stack images, even with our advanced microscope and sensitive camera. 4°C represents a transition temperature, where velocity is high initially but decreases to speeds comparable to those at 1°C–3°C. At 5°C–7°C, velocity is high initially but decreases to very low levels after ~50 min at T_{set} (Figure 2B). This immobilization appears to take effect progressively over time, in contrast to the immediate immobilization at lower temperatures. The velocities at 50–60 min are significantly ($p << 0.001$) below those at 1°C–3°C and near or below our microscope resolution limit. As a result, this minimal velocity (<0.5 μm/s) permits clear submicron-resolution microscopy (see below). Because the final velocities are similar between 5 and 7 °C, we selected 6 °C as the T_{set} for further study.

For animals raised at T_{cult} = 15°C, the strongest immobilization occurs at 1°C after ~30 min (Figure 2C). Nose tip velocity of these animals is comparable to the velocity of animals cultivated at 20°C and immobilized at 5°C–7°C. Immobilization at 2°C and 3°C is progressively less effective than 1°C ($p << 0.001$), and immobilization at 4°C–7°C is inconsistent and generally less effective than at lower temperatures (Figures 2C and 2D). Thus, cultivation temperature strongly impacts immobilization, which is expected given that it alters animal physiology in myriad ways, including modulating their cold habituation.[10]

Different cooling rates produce similar immobilization

We next examined the impact of the cooling rate on immobilization by testing three methods to cool animals down to 6°C at different rates (details in Materials and methods). We term these methods "slow",

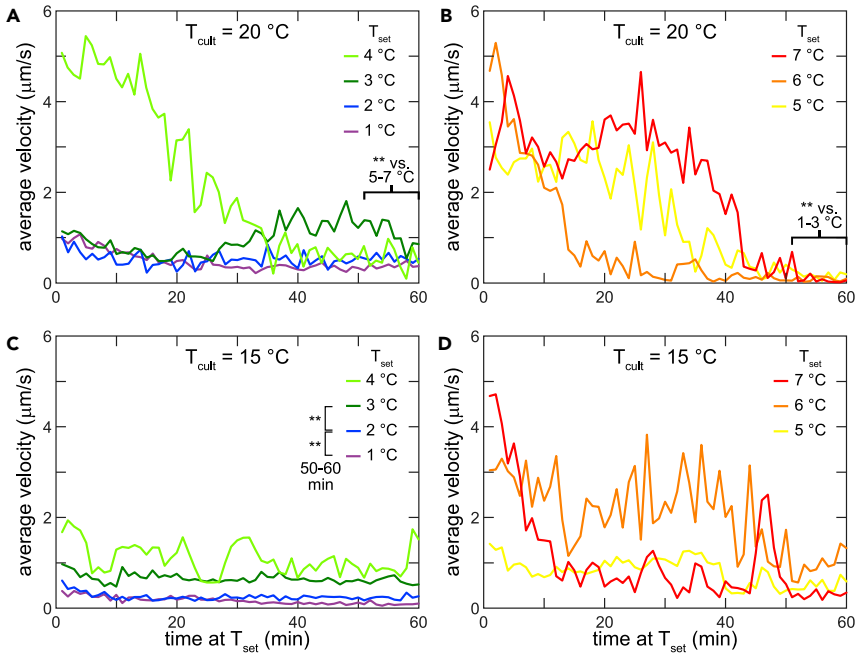

Figure 2. Relatively higher temperatures immobilize 20°C-cultivated animals more effectively

Average nose tip velocity each minute under fast cooling immobilization. (A, C) low and (B, D) high temperature immobilization of animals raised at T_{cult} = 20°C (A, B) and 15°C (C, D). **p < 0.001. n = 6 animals for each condition.

"fast", and "abrupt". Figure S1 shows plate temperature profiles for slow and fast cooling methods. Slow cooling uses a typical 4°C refrigerator to cool down a lidded cultivation plate to 6°C in about 50–60 min. After this first hour in the refrigerator, we transfer this plate to the pre-cooled stage and maintain animals at 6°C. In fast cooling, we place a plate directly onto the cooling stage to bring the plate from 20°C to 6°C. The cooling stage can maintain colder temperatures than the refrigerator; thus, it can cool down animals to 6°C within 15 min. In abrupt cooling, we pick animals from their original 20°C plate directly to a pre-cooled 6°C plate. Based on small animal size and ample thermal conductivity, we expect animals are cooled to 6°C in seconds.

As stated in the section "optimal cooling temperature for immobilization", immobilization at higher T_{set} is strongest starting ~50 min after beginning of cooling. Thus, we measured velocity for an extended length of time, beginning when the animals reached T_{set} and up to 2 h from the start of cooling (Figure 3). We compared abrupt, fast, and slow cooling to 6°C and fast cooling to 1°C. After cooling to 6°C, we observe no significant differences in velocity during the 80–120 min range between slow and fast cooling ($p = 0.08$) or between slow and abrupt cooling ($p = 0.32$), indicating that the cooling rate does not require careful tuning to optimize immobilization. By contrast, in agreement with our prior results (Figure 2), fast cooling to 1°C allows significantly more movement during the 80–120 min range than fast cooling to 6°C ($p < 0.001$).

Slow cooling is the most efficient of the three cooling methods. Abrupt cooling involves the most user time and effort as animals are individually moved. Fast cooling plates idly occupy the stage for an extended time while reaching T_{set}. In contrast, slow cooling occurs in a refrigerator, and animals can be imaged at high resolution immediately after transfer to the cooling stage to maintain T_{set}. Thus, while certain experiments may require fast or abrupt cooling, we favor the efficient slow cooling method and utilize it for the remainder of this study.

Intermittent nose movements under cooling

The goal of our device development is to strongly immobilize animals for imaging, especially for high-resolution microscopy. As such, we ascertained if animals were sufficiently immobilized for imaging by our cooling stage. We quantified nose movements each second to more precisely assess immobilization. Figure 4A shows second-by-second measurements of typical nose movement under 6°C slow cooling. Similar

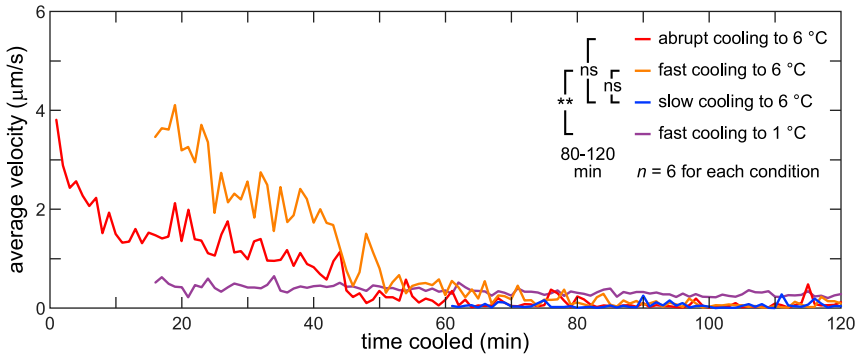

Figure 3. Different cooling rates to 6°C eventually immobilize similarly

Average velocity of nose tip movement for abrupt, fast, and slow cooling methods to 6°C and fast cooling to 1°C. Velocity measurement begins after animals reach T_{set}. n = 6 animals for each condition. **p < 0.001 and not significant (ns) comparisons of movement during 80–120 min.

to sleep and lethargus,[11,12] nose movement under cooling conditions is intermittent, mostly comprised of seconds-long "bouts" of increased activity separated by "windows" with little to no movement. We characterized the distance moved during bouts and the length of the windows. Only 1.4% of movements surpass 1 μm, and 95% of measurements yielded movement below the resolution limit (0.5 μm) (Figure 4B). Movements below 1 μm do not produce visible blur even at the highest magnification of our microscope (64×) because the motion is largely confined to the tip. Also, most of the experiment duration is contained within longer windows: 96% of the duration is part of windows that are longer than 0.5 min, and 90% of the time is part of windows that are longer than 1 min (Figure 4C). This level of movement is sufficiently low to observe by eye and is also amenable to high-resolution, blur-free bright-field imaging by a camera, which can be performed at most time points. Moreover, technology improvements have produced increasingly brighter fluorescent labels, enhanced optics, and efficient cameras. If these tools allow rapid and more sensitive image acquisition, the immobilization requirements may be relaxed. For instance, partial immobilization, achievable at earlier times at 4°C–7°C or all times at 1°C–3°C, may be sufficient for imaging with improved technologies, allowing high-speed repetitive immobilizations for longitudinal imaging. In summary, our cooling immobilization approach reduces animal movement sufficiently to allow clear observation by eye and imaging by camera.

Touch stimulus temporarily reactivates movement

We next investigated the impact of touch stimulus on movement. Gentle and harsh touch to *C. elegans* alters the existing behavior of the animal and provokes an escape response.[8,13,14] Likewise, touching animals in lethargus or sleep also reactivates them.[11,12] We immobilized animals using the slow cooling method to 6°C and stimulated animals by moving them with a pick at 90 min (*i.e.*, harsh touch). As expected, touch stimulus reactivates immobilized animals (Figure S2). Compared to the 10 min before touch stimulus, velocity for the following 10 min is modestly elevated (p = 0.006) before returning to the immobilization baseline during the subsequent 10 min. Thus, if animals are disturbed while immobilized, they may require time before returning to full immobilization.

Animals persist in immobilized state after temperature rises

After a typical experiment involving cooling immobilization, we move plates back to their incubator to return animals to their cultivation temperature. We observed the resumption of movement during warming by turning off the cooling stage. Because animals become strongly immobilized when cooled below 7°C, we expected that movement would return at a similar temperature when warming animals to their cultivation temperature, 20°C. Intriguingly, following slow cooling immobilization and maintenance at 6°C for 1 h, no animals resumed crawling before the plate temperature reached ~10°C. Even after the plate temperature reached 20°C, at least 50% of animals remained immobilized until stimulated by gentle touch, whether externally applied or from contact with other animals moving on the plate. When stimulated by touch, animals transition within a few seconds directly from immobilized to crawling that appears normal as observed by eye. Thus, while animals resume apparently normal behavior following cooling immobilization, the transition from immobilized to crawling may require additional study to fully clarify.

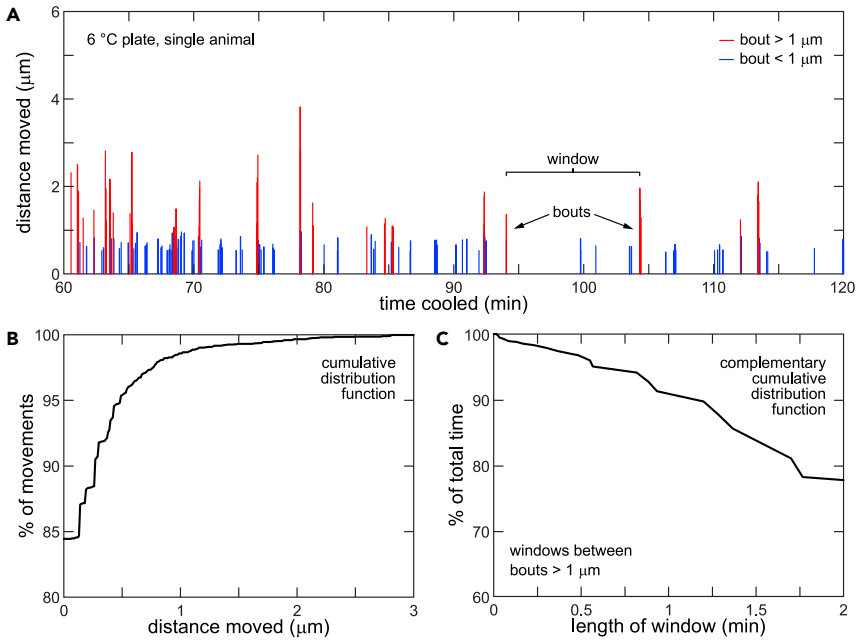

Figure 4. Movement under cooling comprises intermittent bouts with long interstitial windows

(A) Single animal movement measured each second reveals intermittent bouts of increased activity. Movements of <1 μm do not produce significant image blur.

(B) Cumulative distribution function of data in part A. Most movements are small: 99% of movements are <1 μm.

(C) Complementary cumulative distribution function of data in part A. Longer windows comprise most of experiment duration: 96% of duration is part of windows >0.5 min long.

Cooling immobilization does not reduce lifespan or fecundity

Prior studies involving cooling of *C. elegans* indicate that cooling for shorter periods of time does not appear to impact the animal health,[5] but longer periods (>4 h) cause an immediate or progressive decline in health.[10,15] We assayed viability and fecundity of animals immobilized by cooling for 1 h. First, we immobilized animals at 6°C (slow cooling) and quantified their lifespan and number of offspring (Figure S3). Lifespan and fecundity for control and cooled animals are not significantly different (black, blue data). Second, we immobilized animals at 1°C (fast cooling) to test a harsher immobilization condition. Again, lifespan and fecundity for control and cooled animals are not significantly different (light gray, purple data). We conclude that cooling immobilization up to 1 h does not significantly affect animal health.

Time-lapse imaging and 3D image stack

One important application of strong immobilization is to allow high-resolution imaging of fluorescently labeled cells and proteins. Unlike bright-field imaging, fluorescent imaging illuminates animals with high-intensity light, which stimulates movement in some animals. We observed this light-stimulated movement to ascertain if cooling immobilization is sufficient for high-resolution fluorescence imaging. With our setup and animal strains, we note increased movement primarily when the illumination is focused to a size less than the animal length. Our current investigations are aimed at quantifying and minimizing this effect. By eye, the nose appears to be more sensitive than the tail or the body to light. The specific cell(s) expressing GFP affect light sensitivity as FLP neuron-fluorescent animals can be illuminated with >10× more light intensity than ASJ neuron-fluorescent animals before stimulating movement, even though both are in the nose. Also, green light illumination (red fluorescence imaging) triggers much less movement than blue light (green fluorescence imaging). These gradations of sensitivity are consistent with prior findings that neurons in the nose, and particularly the ASJ, contribute strongly to wavelength-dependent light sensitivity in *C. elegans*.[16] Under illumination intensities sufficient for fluorescence imaging, most animals remain motionless for tens of second to minutes, allowing clear high-resolution z stack imaging throughout the animal.

Incompletely immobilized animals produce images with blurred features due to motion during or between images. By imaging individual neurons in immobilized animals, we demonstrate the capacity of our cooling

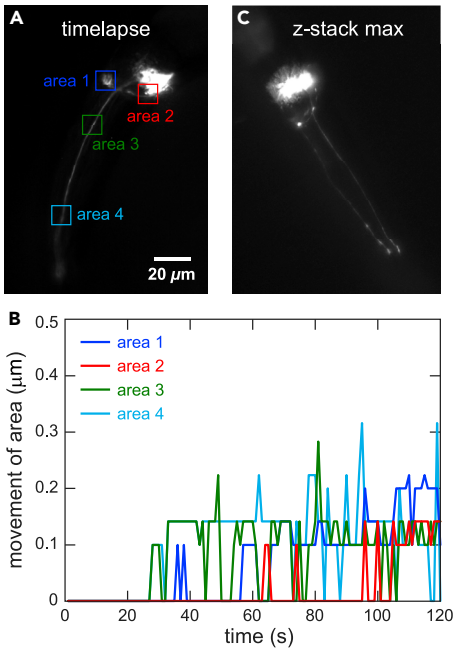

Figure 5. High-resolution imaging of individual animal under 6°C cooling immobilization

Fluorescent *C. elegans* ASJ neuron imaged at 64× magnification.

(A) Maximum projection of 2-min time-lapse image sequence shows no motion blur. Relative movement of structures in areas 1–4 tracked by cross-correlation.

(B) Minimal movement of structures in areas 1–4 during time-lapse.

(C) Maximum projection of 3D image stack acquired manually. Structures show no motion blur. Scale bars: 20 μm (A, C).

stage to allow high-resolution time-lapse and z stack fluorescence images of fine features without movement-induced blurring. To quantify motion within the imaging window, we obtained time-lapse recordings (2 min length, 1 frame/s, 100-ms exposure) of an ASJ neuron expressing GFP. By cross-correlation, we tracked the movement of neuron structures within four areas in the field of view that focused on portions of the neuron (Figure 5A). The distance the neuron structures moved from their original position is shown in Figure 5B and is usually less than 0.2 μm, which is below our resolution limit of 0.5 μm and does not introduce motion blur to the image.

We also took a z stack of the ASJ neuron comprising 41 slices with 1 μm step size taken at 1 slice every 4 s. As shown by the maximum projection of the z stack in Figure 5C, while there is haze around neuron structures from inherent out-of-focus and scattered light in widefield imaging,[17] there is no image blur from motion. Specifically, the neuronal fibers are clearly resolved, even at high resolution. This clear image indicates minimal animal movement during 160 s of imaging, and it underscores the effectiveness of our instrument and approach for immobilization even while strongly illuminating for fluorescence imaging.

Embryo imaging

Immobilizing *C. elegans* embryos can be challenging due to their protective eggshell. We demonstrated that cooling immobilizes embryos sufficiently to produce clear 3D images. Prior studies immobilized embryos by low temperature,[18] mechanical trapping,[19] and chemical anesthetics.[20] While *C. elegans* embryos cannot move any appreciable distance, they rotate and twitch within the eggs. Therefore, we can quantify movement and assess the quality of embryo imaging with and without cooling. We imaged embryos for extended times without cooling and found that animal movement within a 200-ms exposure time blurs cell bodies and precludes clear imaging of small or thin structures, such as neuronal fibers (Figures 6A and 6C). Embryo cells also move between successive images, so images cannot be aligned or observed with extended time imaging such as time-lapse or z-stacks (Figures 6B and 6D). We then imaged embryos with slow cooling to 6°C and found that animal movement was profoundly reduced. There was minimal movement even over timescales >30 s, allowing clear imaging of neuronal fibers in a single exposure time (Figures 6E and 6G) and precise alignment of successive images (Figures 6F and 6H). These timescales are sufficiently long enough to permit acquisition of z-stacks for visualizing 3D structures.

Cooling immobilization largely eliminates animal processing time

To assess the capacity of our cooling approach to accelerate imaging experiments, we measured time spent imaging 100 animals under standard azide immobilization[21,22] and under cooling immobilization.

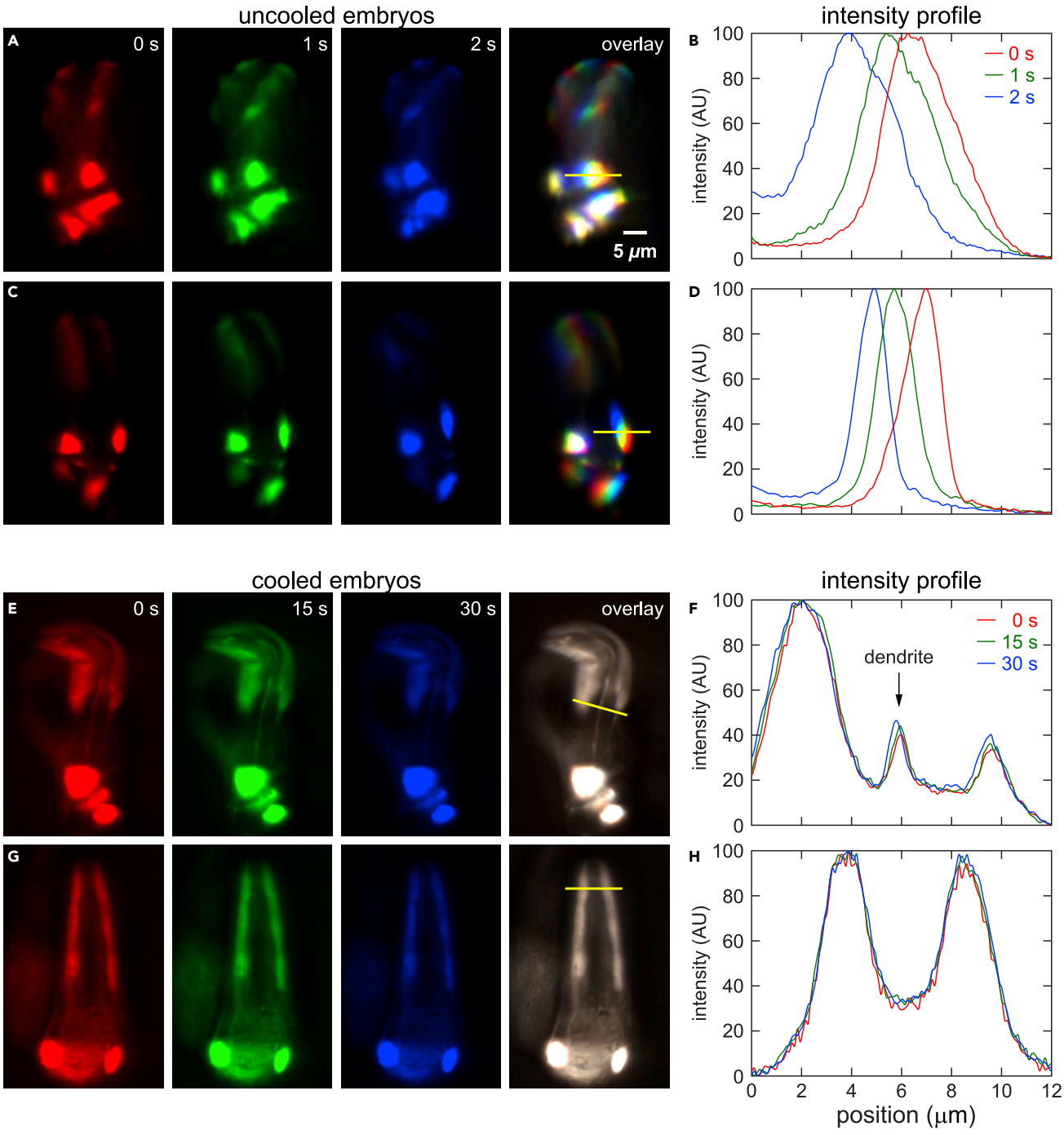

Figure 6. Cooling immobilizes embryo for clear imaging without motion blurring

False-colored fluorescence images of embryo nose (A, C, E, G) and intensity plot profile (B, D, F, H).

(A, C) Images taken at 1 s intervals of uncooled embryo. Overlay and profile shows motion blurring.

(E, G) Images taken at 15 s intervals of cooled embryo. Overlay and profile indicates that movement is below resolution limit (0.5 μm). Scale bars: 5 μm (A, C, E, G).

We choose azide immobilization by two reasons. First, azide immobilization is a standard approach and widely used in imaging *C. elegans*. Second, the effectiveness of our cooling immobilization is more similar to azide immobilization than other immobilization techniques.

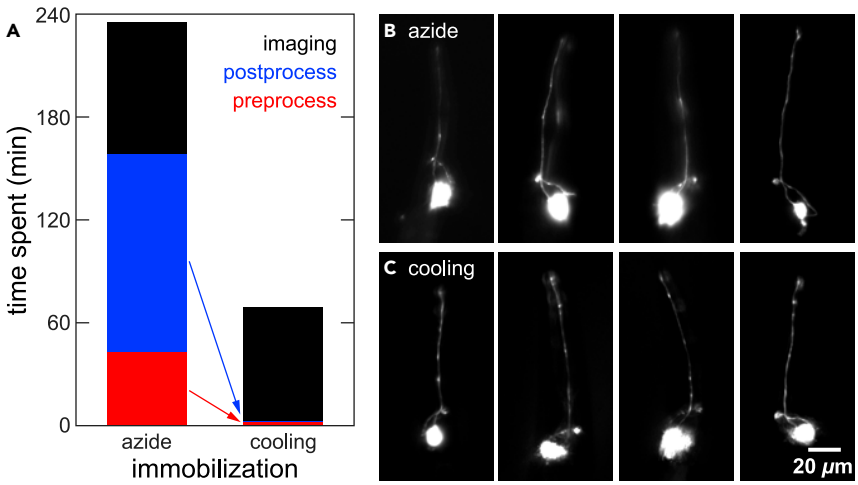

Figure 7. Cooling immobilization reduces non-imaging time by 98%

Animals fluorescently imaged under typical azide or cooling immobilization, n = 100 each.

(A) Time spent on preprocessing, imaging, and postprocessing steps. Preprocessing includes making agar-azide solution, fabricating slides, mounting animals, and moving plates. Postprocessing includes recovering animals, removing azide, moving plates. Selected images of ASJ neuron in animal nose under azide (B) and cooling (C) immobilization. Both strategies introduce no motion blur. Scale bars: 20 μm (B, C).

Azide immobilization requires an involved and time-consuming procedure, which is further extended if animal recovery is required. As shown in Figure 7A and detailed in Table 1, high-resolution single-neuron imaging of 100 animals (selected images in Figure 7B) requires about 4 h of user effort in total. However, the time actually spent on imaging (Figure 7A, black bar) is only 1/3rd of the total time. The remainder of the time is spent on pre- and postprocessing (red and blue bars), including making agar-azide solution, fabrication of azide slides, mounting and dismounting animals, recovering animals in buffer to remove the anesthetic, and moving animals back to their cultivation plates. Cooling immobilization eliminates nearly all the pre- and postprocessing steps of azide immobilization, reducing the non-imaging time by over 98% (Figure 7A). Total experimental time is reduced by over 70%, while imaging quality was comparable (selected images in Figure 7C). As further described in the methods, we believe the timescales measured in our experiment are representative of typical imaging experiments.[23] Thus, cooling immobilization greatly accelerates the pace of imaging experiments.

Cooling immobilization rapidly assays genes underlying conditioned regeneration

Our laboratory studies neuroregeneration and, in a parallel study, identified that the expression of the gene, *thioredoxin-1* (TXN/*trx-1*), roughly correlates with regenerative capacity.[24] A fluorescent GFP reporter of *trx-1* potentially allows high-throughput screening of regeneration genes without time--consuming surgery needed in previous studies. We are specifically interested in genes underlying lesion-conditioned regeneration,[25] which is distinct from other forms of neuronal regeneration mediated by the well-studied gene dual leucine zipper kinase DLK/*dlk-1*.[26] Several pathways underlie conditioned regeneration, including a sensory activity pathway and a cyclic adenosine monophosphate (cAMP) pathway.[23] The sensory pathway includes the beta subunit of a cyclic nucleotide-gated channel CNGB/*tax-2*, whose mutation strongly stimulates conditioned regeneration and upregulates *trx-1*:*gfp*. The cAMP response element-binding protein, CREB/*crh-1*, is potentially downstream of both pathways, but its role in conditioned regeneration is unclear.

The fluorescence of *tax-2* and *tax-2*; *crh-1* mutants are very similar and indistinguishable by eye; however, by measuring fluorescence in >800 animals using the cooling platform (Figure 8A, black bars), we found that *crh-1* mutation significantly reduces *tax-2*-enhanced fluorescence. Animals must be immobilized to ensure that the similar fluorescence levels are accurately measured and distinguished. Immobilization avoids blurring and out-of-focus imaging which reduces apparent fluorescence. Our Copli instrument significantly expedites this fluorescence quantification: imaging fluorescence for >800 animals immobilized by cooling consumed ~1.5 h of user effort. In contrast, based on our prior experience, we estimate that

Table 1. Cooling immobilization eliminates bulk of pre- and postprocessing time

	Agar pad immobilization		Cooling immobilization	
	Process	Time (min)	Process	Time (min)
	make agar solution with azide	14.1		
	fabricate agar pads	1.3	transfer plates to refrigerator	1.0
	cool agar pads	2.9	turn on cooling stage	1.0
batch #1	mount on slide	5.7		
	image slide	**20.3**	**image plate**	**17.1**
	recover in buffer	21.7		
	transfer to plate	6.8		
batch #2	mount on slide	6.3		
	image slide	**20.8**	**image plate**	**15.3**
	recover in buffer	21.9		
	transfer to plate	6.8		
batch #3	mount on slide	6.1		
	image slide	**18.2**	**image plate**	**16.6**
	recover in buffer	22.6		
	transfer to plate	6.2		
batch #4	mount on slide	6.7		
	image slide	**17.3**	**image plate**	**17.1**
	recover in buffer	21.7		
	transfer to plate	6.8		
	transfer plates to incubator	1.0	transfer plates to incubator	1.0
	preprocessing time	43.1		2.0
	postprocessing time	115.5		1.0
	imaging time	**76.5**		**66.1**
	total	235.1		69.1

We imaged four batches of 25 animals each for both procedures. Preprocessing includes mounting animals and steps listed prior to the batches. All imaging steps are bolded. Postprocessing time includes recovering animals, transferring animals, and transferring plates.

imaging animals mounted onto agar-azide pads would require >5× more time. After observing a reduction in fluorescence, we noted that *crh-1* mutation reduces *tax-2*-enhanced ectopic axon outgrowth (Figure 8A, light gray bars), which has an overlapping genetic pathway with conditioned regeneration.[23] Finally, direct laser ablation of the ASJ neuron in *dlk-1* mutants shows that *crh-1* reduces frequency of conditioned regeneration (Figures 8B and 8C). While prior studies indicate that *crh-1* does not underlie a different form of regeneration,[27] our results demonstrate that CREB/*crh-1* functionally underlies conditioned regeneration. Thus, the cooling stage enables rapid identification of a novel regeneration gene by changes in fluorescence that are only detectable by immobilizing and quantitatively measuring a large population.

DISCUSSION

Envisioned workflows

We envision two potential workflows that utilize our cooling approach to enable convenient, reversible immobilization of many animals for high-resolution imaging. In this study, we demonstrated the first workflow, where entire cultivation plates are cooled to 6°C. Because this method requires ~50 min to maximally immobilize animals, plates are "pre-cooled" by placing them in a 4°C refrigerator for ~1 h, and subsequent cooling on the stage maintains the immobilization temperature. To maximize efficiency in multi-plate experiments, a plate is processed on the stage while simultaneously pre-cooling the next plate that will be processed. Following imaging of immobilized animals, plates are returned directly to their incubator to bring them back to their cultivation temperature. The second workflow, involving a microchamber device for longitudinal imaging, is further described in the "future developments and applications" section below.

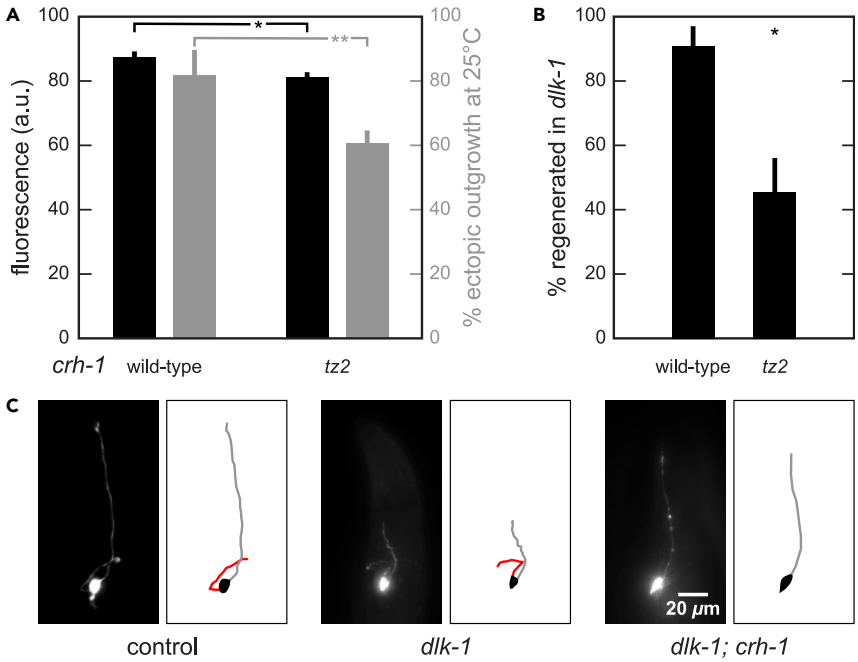

Figure 8. Cooling immobilization enables identification of neuroregeneration gene

Mutation of *crh-1* significantly reduces (A) ASJ cell body fluorescence (black) and frequency of ectopic axon outgrowth (light gray) in *tax-2* strains and (B) frequency of ASJ-conditioned regeneration.

(C) Control and postsurgery GFP fluorescence images and line drawings of ASJ neuron with axon (red), dendrite (gray), and cell body (black). Control image replicated from Figure 7B n ≥ 386 (fluorescence), 158 (outgrowth), 20 (regeneration). *p < 0.05, **p < 0.001. The fluorescence data in (A) are represented as mean ± SE of mean (SEM). The ectopic outgrowth in (A) and the regenerated in *dlk-1* in (B) are represented as mean ± SD. Scale bar: 20 µm (C).

Advantages of cooling stage and approach

The Copli instrument and approach have several technical capabilities, including some significant improvements over prior immobilization methods. First, large *C. elegans* populations are readily and reversibly immobilized by cooling, allowing observation, imaging, screening, and manipulation of many animals over long time periods. Some effects, including weakly penetrant defects, are difficult to observe in individual animals. The capacity to rapidly observe large populations of animals at high resolution enables us to clearly see the effect of mutations and interventions. Second, for some applications or genetic backgrounds, immobilization by cooling may be preferable to other methods due to their secondary effects, such as stress response.[6] For instance, chemical agents such as sodium azide induce stress proteins and thermotolerance in *C. elegans*.[28] Third, our stage permits high-resolution fluorescence imaging of animals directly on cultivation plates. While *in vivo* microscopy on cultivation plates has been a mainstay technique for decades, it is more often performed by eye and at lower resolution. Our approach enables the study of subcellular processes and cell morphology without manipulating individual animals. Fourth, optical transparency of the sapphire window allows easy observation and imaging by bright-field transillumination, which is a primary method used for many imaging applications in *C. elegans*. Fifth, we designed our cooling stage for straightforward insertion into or removal from common upright microscope setups. The cooling stage is applicable to a variety of setups including widefield epifluorescence, confocal, two-photon, and bright-field microscopes. The compact stage is simply placed under the objective on the stage of the microscope (Figure 1C), and the cultivation plate rests directly onto the cooling stage. Redesigning the stage to flip over could allow imaging on inverted microscope setups. Our cooling approach is also amenable to typical *C. elegans* experimental workflows involving solid media cultivation. Finally, most immobilization techniques for high-resolution imaging do not easily allow animal reorientation while imaging. Our cooling stage maintains access to animals, which can be manipulated by a standard platinum pick throughout imaging, at the cost of time to reestablish full immobilization (see "touch stimulus" section above). These technical capabilities enable broad application of our device and approach to many experiments that require high-resolution *in vivo* microscopy on large numbers of animals.

The Copli instrument and approach also have three practical, user-friendly features. First, our approach requires minimal user effort. Most other reversible immobilization techniques require transfer and manipulation of individual animals to complex setups or slides, which must also be fabricated. Our approach obviates this work by immobilizing animals on their cultivation plate. For high-resolution imaging experiments that involve animal recovery, two-thirds of the experimental time involves non-imaging activities such as animal handling, immobilization, and recovery (Figure 7A and Table 1). Our full sodium azide immobilization procedure[21] requires ~160 min to process four batches of 25 animals each, not including time spent on imaging animals. Our cooling immobilization procedure requires ~3 min, representing a savings of >98% of the time expended on non-imaging activities. Thus, our approach greatly accelerates the pace of experiments, enabling the straightforward application of high-resolution imaging to challenging procedures, such as screens. Moreover, because plates hold more animals than slides, cooling immobilization has better economies of scale compared to conventional immobilization. Second, our cooling stage and approach are very simple and straightforward, and they require minimal training to operate. Some immobilization techniques involve complex setups or procedures and thus require significant training and fine-tuning. In contrast, our cooling stage has only a single voltage adjustment to control the immobilization temperature. Thus, our approach's simplicity makes it intuitive as well as resistant to failure. Finally, our device is accessible and inexpensive: we assembled it from easily attainable and affordable components, totaling a cost of ~$500. In summary, our device and approach have significant technical capabilities in a very user-friendly design.

Potential applications

Our cooling stage can immobilize *C. elegans* for bright-field or fluorescence imaging of the entire animal as well as many tissues, cells, and subcellular structures. Bright-field applications include manipulation and sorting of animals based on gross morphology. Fluorescence applications include visualization of the presence or precise localization of fluorescent protein, stains, and labels. Animals can be observed by eye or imaged by camera, allowing quantification of fluorescent markers in and across images. Applications involving many animals are particularly empowered by our cooling stage. One such group of applications are visual screens, which often involve observation of live animals on their cultivation plates without any immobilization. However, observing differences in morphology, phenotype, or brightness of a fluorescence marker (especially at high resolution) is significantly easier, and sometimes only possible, when animals are immobilized. For example, we mimicked a fluorescence-based screen (Figure 8A) to assess the role of *crh-1* in lesion conditioning. Because the fluorescence levels of *tax-2* and *tax-2; crh-1* are so similar, it is only by immobilizing, imaging many animals, and quantitatively measuring fluorescence with a camera, that we can demonstrate a significant difference.

Key technical developments and new findings

In our study, we develop a new, compact thermoelectric stage that cools entire cultivation plates to immobilize populations of *C. elegans* for imaging. Our stage cools plates to a uniform temperature distribution across the agar surface that is stable over long time periods. We describe animal movement under many cooling conditions in far greater detail than previously reported. We demonstrate that cooling has minimal impact on lifespan and fecundity. Our cooling stage successfully immobilizes animals sufficiently to allow high-resolution bright-field imaging. Despite some movement arising from high-intensity illumination for high-resolution fluorescence imaging, we demonstrate the capacity of our immobilization approach to perform blur-free time-lapse and z stack fluorescence imaging. In summary, our cooling stage represents a novel and effective way to reversibly immobilize large populations of *C. elegans* for high-resolution bright-field and fluorescence imaging.

During our study, we also encountered some interesting and unusual animal behavior. First, previous studies immobilized animals between 2°C and 4°C.[5,7] By careful and systematic assay, we find that optimal immobilization of *C. elegans* occurs at a counterintuitively higher temperature of 5°C–7°C after animals have been cooled for ~50 min. In contrast, animals cooled to 1°C–3°C maintain a relatively stable level of movement that is significantly higher than at 6°C. Animals held at 1°C only slightly reduce their movement even after 2 h. In fact, a higher immobilization temperature is preferable as it is easier to maintain, has lower risk of freezing animals, and is presumably a more benign environment. Second, animal behavior under cooling and under sleep shares some characteristics. Similar to sleep, animals immobilized by cooling spontaneously switch periods of movement and quiescence. After cooling immobilization, many animals persist in the immobilized state even after warmed to cultivation temperatures but resume normal movement rapidly following gentle touch. Further studies are required to determine if cooling immobilization exhibits other hallmarks of sleep, or if it is more akin to partial anesthesia.

Limitations of the study

There are several limitations of our approach. First, animals raised at 15°C are immobilized at a lower temperature compared to worms raised at 20°C, indicating that cultivation temperature modulates cooling immobilization. This is not unexpected as prior studies have shown that raising *C. elegans* at colder temperatures improves cold tolerance.[29] Thus, additional fine-tuning of our approach is required if animals are not cultivated at 20°C. Likewise, we also speculate that some temperature-sensitive mutant strains of *C. elegans* may require adjustment of immobilization temperature, as we have optimized our approach for the wild-type background. Second, the speed of immobilization (~50 min) is slower than most other methods, but we expect that the easy step of pre-cooling plates overcomes this weakness for most applications. Third, imaging fine structures at locations that exhibit relatively more movement, such as the dendritic cilia at the nose tip, could be challenging. Finally, high-intensity illumination for fluorescence imaging at high resolution stimulates movement in some animals and may require adjusting illumination intensity and exposure time to minimize animal movement while maximizing experimental speed.

Future developments and applications

Our cooling approach and platform could be developed in several ways to greatly enhance its capabilities. A microfluidic or microchamber[30] device utilized with our cooling approach could permit longitudinal imaging of individual animals. A thin device would enable rapid, repeated cooling for brief imaging windows with minimal impact on animal health.[5] Such a device would be useful for tracking development or neuroregeneration following injury. In our study, we also completed procedures manually, but one advantage of our approach is that it is amenable to automation. Commercial plate handlers can move plates to instruments and could be easily adapted to load plates onto our cooling stage. The cooling immobilization and imaging could also be automated through multiple coolers and translation stages. There is also great potential for integrating our approach with image processing and segmentation algorithms to enable automated recognition of cellular components and targeting for laser surgery. Accelerating the imaging by itself, however, would not reduce the substantial amount of time spent on non-imaging activities, highlighting the need to develop immobilization platforms to fully exploit automation. The developments listed above would significantly extend the capabilities and accelerate the throughput of our platform, allowing its application to a wide array of questions that are currently unapproachable.

STAR★METHODS

Detailed methods are provided in the online version of this paper and include the following:

- KEY RESOURCES TABLE
- RESOURCE AVAILABILITY
  - Lead contact
  - Materials availability
  - Data and code availability
- EXPERIMENTAL MODEL AND SUBJECT DETAILS
  - Animals
- METHOD DETAILS
  - Device design, components and assembling
  - Plate temperature measurements
  - Cooling methods: slow, fast, and abrupt
  - Slow cooling
  - Fast cooling
  - Abrupt cooling
  - Tip-tracking
  - Lifespan and fecundity analysis
  - Lifespan
  - Fecundity
  - Fluorescence imaging
  - Measurement of time expenditure for azide and cooling immobilization
  - Fluorescence, ectopic outgrowth, and regeneration measurements
- QUANTIFICATION AND STATISTICAL ANALYSIS

SUPPLEMENTAL INFORMATION

Supplemental information can be found online at https://doi.org/10.1016/j.isci.2023.105999.

ACKNOWLEDGMENTS

We thank the members of the Chung Laboratory for feedback on the manuscript. We thank Neil Patel, Claire Ma, and Phillip Wible (Bioengineering, Northeastern Univ.) for assistance with animal nose tip tracking. We acknowledge Max Heiman (Genetics, Children's Hospital Boston) for providing CHB4526 for embryonic imaging and Antonio Miranda-Vizuete (Biomedicine Institute of Sevilla, Seville, Spain) for providing VZ126 to generate strains for regeneration studies. We acknowledge Wenchao Zhu (Mechanical Engineering, Northeastern Univ.) for technical support in thermal distribution measurement. We acknowledge Xin Sun (Bioengineering, Northeastern Univ.) for technical support in 3D printing.

AUTHOR CONTRIBUTIONS

Several people contributed to the work described in this paper. S.H.C. conceived the idea. Y.L.W., E.L.J., and L.G.S. designed, constructed, and characterized the stage. Y.L.W. assessed imaging quality and recorded animal movement. Y.L.W. and E.L.J. analyzed video recordings. E.L.J. and N.W.F.G. performed lifespan and fecundity experiments. Y.L.W. and N.W.F.G. assessed experimental speed. N.W.F.G. carried out CREB experiments; N.W.F.G. and E.L.J. analyzed CREB data and assessed cooling impact on animal healthspan. S.H.C. supervised the experiments and the development of the manuscript. E.L.J. and S.H.C. wrote the first draft of the manuscript; all authors subsequently took part in the revision process and approve the final copy of the manuscript.

DECLARATION OF INTERESTS

The authors declare no competing interests.

Received: March 16, 2022
Revised: November 19, 2022
Accepted: January 12, 2023
Published: February 17, 2023

REFERENCES

1. Reeve, E.C.R. (1988). The Nematode Caenorhabditis elegans . Edited by William B. Wood and the Community of C. elegans Researchers. New York: cold Spring Harbor Laboratory, 1988. 667 pages. US $97.00. ISBN 0 87969 307 X. Genet. Res. *52*, 243–244. https://doi.org/10.1017/S0016672300027713.

2. Kim, E., Sun, L., Gabel, C.V., and Fang-Yen, C. (2013). Long-Term Imaging of Caenorhabditis elegans Using Nanoparticle-Mediated Immobilization. PLoS One *8*, e53419. https://doi.org/10.1371/journal.pone.0053419.

3. Guo, S.X., Bourgeois, F., Chokshi, T., Durr, N.J., Hilliard, M.A., Chronis, N., and Ben-Yakar, A. (2008). Femtosecond laser nanoaxotomy lab-on-a-chip for in vivo nerve regeneration studies. Nat. Methods *5*, 531–533. https://doi.org/10.1038/nmeth.1203.

4. Zeng, F., Rohde, C.B., and Yanik, M.F. (2008). Sub-cellular precision on-chip small-animal immobilization, multi-photon imaging and femtosecond-laser manipulation. Lab Chip *8*, 653–656. https://doi.org/10.1039/B804808H.

5. Rohde, C.B., and Yanik, M.F. (2011). Subcellular in vivo time-lapse imaging and optical manipulation of Caenorhabditis elegans in standard multiwell plates. Nat. Commun. *2*, 271. https://doi.org/10.1038/ncomms1266.

6. Manjarrez, J.R., and Mailler, R. (2020). Stress and timing associated with Caenorhabditis elegans immobilization methods. Heliyon *6*, e04263. https://doi.org/10.1016/j.heliyon.2020.e04263.

7. Chung, K., Crane, M.M., and Lu, H. (2008). Automated on-chip rapid microscopy, phenotyping and sorting of C. elegans. Nat. Methods *5*, 637–643. https://doi.org/10.1038/nmeth.1227.

8. Alkema, M.J., Hunter-Ensor, M., Ringstad, N., and Horvitz, H.R. (2005). Tyramine Functions Independently of Octopamine in the Caenorhabditis elegans Nervous System. Neuron *46*, 247–260. https://doi.org/10.1016/j.neuron.2005.02.024.

9. Chung, S.H., Schmalz, A., Ruiz, R.C.H., Gabel, C.V., and Mazur, E. (2013). Femtosecond Laser Ablation Reveals Antagonistic Sensory and Neuroendocrine Signaling that Underlie C. elegans Behavior and Development. Cell Rep. *4*, 316–326. https://doi.org/10.1016/j.celrep.2013.06.027.

10. Ohta, A., Ujisawa, T., Sonoda, S., and Kuhara, A. (2014). Light and pheromone-sensing neurons regulates cold habituation through insulin signalling in Caenorhabditis elegans. Nat. Commun. *5*, 4412. https://doi.org/10.1038/ncomms5412.

11. Raizen, D.M., Zimmerman, J.E., Maycock, M.H., Ta, U.D., You, Y.J., Sundaram, M.V., and Pack, A.I. (2008). Lethargus is a Caenorhabditis elegans sleep-like state. Nature *451*, 569–572. https://doi.org/10.1038/nature06535.

12. Iwanir, S., Tramm, N., Nagy, S., Wright, C., Ish, D., and Biron, D. (2013). The Microarchitecture of C. elegans Behavior during Lethargus: Homeostatic Bout Dynamics, a Typical Body Posture, and Regulation by a Central Neuron. Sleep *36*, 385–395. https://doi.org/10.5665/sleep.2456.

13. Chalfie, M., Hart, A.C., Rankin, C.H., and Goodman, M.B. (2014). Assaying mechanosensation. WormBook. https://doi.org/10.1895/wormbook.1891.1172.1891.

14. Chalfie, M., and Sulston, J. (1981). Developmental genetics of the mechanosensory neurons of Caenorhabditis elegans. Dev. Biol. *82*, 358–370. https://doi.org/10.1016/0012-1606(81)90459-0.

15. Robinson, J.D., and Powell, J.R. (2016). Long-term recovery from acute cold shock in Caenorhabditis elegans. BMC Cell Biol. *17*, 2. https://doi.org/10.1186/s12860-015-0079-z.

16. Ward, A., Liu, J., Feng, Z., and Xu, X.Z.S. (2008). Light-sensitive neurons and channels mediate phototaxis in C-elegans. Nat. Neurosci. *11*, 916–922. https://doi.org/10.1038/nn.2155.

17. Wang, Y.L., Grooms, N.W.F., Civale, S.C., and Chung, S.H. (2021). Confocal imaging capacity on a widefield microscope using a spatial light modulator. PLoS One *16*, e0244034. https://doi.org/10.1371/journal.pone.0244034.

18. Rabin, Y., and Podbilewicz, B. (2000). Temperature-controlled microscopy for imaging living cells: apparatus, thermal analysis and temperature dependency of embryonic elongation in Caenorhabditis elegans. J. Microsc. *199*, 214–223. https://doi.org/10.1046/j.1365-2818.2000.00720.x.

19. Cornaglia, M., Mouchiroud, L., Marette, A., Narasimhan, S., Lehnert, T., Jovaisaite, V., Auwerx, J., and Gijs, M.A.M. (2015). An automated microfluidic platform for C. elegans embryo arraying, phenotyping, and long-term live imaging. Sci. Rep. *5*, 10192. https://doi.org/10.1038/srep10192.

20. Podbilewicz, B., and Gruenbaum, Y. (2006). Live Imaging of Caenorhabditis elegans: preparation of samples. CSH Protoc. *2006*. pdb.prot4601. https://doi.org/10.1101/pdb.prot4601.

21. Bargmann, C.I., and Avery, L. (1995). Laser killing of cells in Caenorhabditis elegans. Methods Cell Biol. *48*, 225–250. https://doi.org/10.1016/s0091-679x(08)61390-4.

22. Chung, S.H., Clark, D.A., Gabel, C.V., Mazur, E., and Samuel, A.D.T. (2006). The role of the AFD neuron in C. elegans thermotaxis analyzed using femtosecond laser ablation. BMC Neurosci. *7*, 30. https://doi.org/10.1186/1471-2202-7-30.

23. Chung, S.H., Awal, M.R., Shay, J., McLoed, M.M., Mazur, E., and Gabel, C.V. (2016). Novel DLK-independent neuronal regeneration in Caenorhabditis elegans shares links with activity-dependent ectopic outgrowth. Proc. Natl. Acad. Sci. USA *113*, E2852–E2860. https://doi.org/10.1073/pnas.1600564113.

24. Grooms, N.W.F., Fitzgerald, M.Q., Schulting, L.G., Ureña, S.E., and Chung, S.H. (2022). Expression of thioredoxin-1 in the ASJ neuron corresponds with and enhances intrinsic regenerative capacity under lesion conditioning in *C. elegans*. Preprint at bioRxiv. https://doi.org/10.1101/2022.09.19.508543.

25. Richardson, P.M., and Issa, V.M. (1984). Peripheral Injury Enhances Central Regeneration of Primary Sensory Neurons. Nature *309*, 791–793. https://doi.org/10.1038/309791a0.

26. Hammarlund, M., Nix, P., Hauth, L., Jorgensen, E.M., and Bastiani, M. (2009). Axon Regeneration Requires a Conserved MAP Kinase Pathway. Science *323*, 802–806. https://doi.org/10.1126/science.1165527.

27. Ghosh-Roy, A., Wu, Z., Goncharov, A., Jin, Y., and Chisholm, A.D. (2010). Calcium and Cyclic AMP Promote Axonal Regeneration in Caenorhabditis elegans and Require DLK-1 Kinase. J. Neurosci. *30*, 3175–3183. https://doi.org/10.1523/JNEUROSCI.5464-09.2010.

28. Massie, M.R., Lapoczka, E.M., Boggs, K.D., Stine, K.E., and White, G.E. (2003). Exposure to the metabolic inhibitor sodium azide induces stress protein expression and thermotolerance in the nematode Caenorhabditis elegans. Cell Stress Chaperones *8*, 1–7. https://doi.org/10.1379/1466-1268(2003)8<1:ETTMIS>2.0.CO;2.

29. Murray, P., Hayward, S.A.L., Govan, G.G., Gracey, A.Y., and Cossins, A.R. (2007). An explicit test of the phospholipid saturation hypothesis of acquired cold tolerance in Caenorhabditis elegans. Proc. Natl. Acad. Sci. USA *104*, 5489–5494. https://doi.org/10.1073/pnas.0609590104.

30. Bringmann, H. (2011). Agarose hydrogel microcompartments for imaging sleep- and wake-like behavior and nervous system development in Caenorhabditis elegans larvae. J. Neurosci. Methods *201*, 78–88. https://doi.org/10.1016/j.jneumeth.2011.07.013.

31. Schneider, C.A., Rasband, W.S., and Eliceiri, K.W. (2012). NIH Image to ImageJ: 25 years of image analysis. Nat. Methods *9*, 671–675.

32. Brenner, S. (1974). The genetics of Caenorhabditis elegans. Genetics *77*, 71–94. https://doi.org/10.1093/genetics/77.1.71.

33. Larsen, P.L., Albert, P.S., and Riddle, D.L. (1995). Genes that regulate both development and longevity in Caenorhabditis elegans. Genetics *139*, 1567–1583. https://doi.org/10.1093/genetics/139.4.1567.

STAR★METHODS

KEY RESOURCES TABLE

REAGENT or RESOURCE	SOURCE	IDENTIFIER
Experimental models: Organisms/strains		
CHB4256	Heiman Lab, Boston Children's Hospital	*hmnEx2428[pIM48(pegl-13::gfp) + pRF4(rol-6(su1006))]*
N2	Caenorhabditis Genetics Center	
BOS51	This paper	*crh-1(tz2)III; dlk-1(ju476)I; vzEx29[p285(Pssu-1::GFP) + pRF4(rol-6(su1006)]*
BOS52	This paper	*dlk-1(ju476)I; vzEx29[p285(Pssu-1::GFP) + pRF4(rol-6(su1006)]*
BOS60	This paper	*tax-2(p691)I; crh-1(tz2)III; ofIs1[ptrx-1::trx-1::gfp]*
BOS72	Chung et al.[23]	*tax-2(p691)I; ofIs1[ptrx-1::trx-1::gfp]*
BOS84	Chung et al.[23]	*daf-11(sa195)V; jhEx560[ptrx::trx-1::gfp]*
Software and algorithms		
ImageJ/FIJI	Schneider et al.[31]	https://imagej.nih.gov/ij/; RRID:SCR_002285
Matlab 2020b	Mathworks Inc.	https://www.mathworks.com/products/new_products/release2020b.html; RRID:SCR_001622
SolidWorks 2022	Dassault Systems	https://www.solidworks.com/product/whats-new-2022
Other		
Peltier heat pump	CUI Devices	CP854705-2
Copper block	Third party source	Machined to 100x140x3 mm
Sapphire window	Altos Photonics	Call Altos for custom order (80 mm diameter, 3 mm thick)
Thermal paste	Florence	Arctic MX-4
Water cooling pump	Yosoo	SC-300T
Copper cooling block	Unbranded	40x40x10mm
Water cooling radiator	DIYhz	12 Pipe 240 mm with double fans
Silicone tubing	ThermoFisher	Nalgene 50
Custom installation bracket	This paper	3D printing polylactide filament
Widefield fluorescence stereomicroscope	Leica	M205
Camera for microscopy images	Oxford Instrument	Andor Zyla 4.2 sCMOS
3-axis stage for z-stacks	Thorlabs	MBT616D
Thermal camera	Teledyne	Flir C2
Digital thermocouple	Proster Trading Limited	Model#4333090752

RESOURCE AVAILABILITY

Lead contact

Further information and requests for resources and materials may be directed to lead contact, Prof. Samuel Chung (schung@northeastern.edu).

Materials availability

This study did not generate new unique reagents or materials.

Data and code availability

- All data produced in this study are included in the published article and its supplementary information, or are available from the lead contact upon request.

- This paper does not report original code.
- Any additional information required to reanalyze the data reported in this paper is available from the lead contact upon request.

EXPERIMENTAL MODEL AND SUBJECT DETAILS

Animals

We maintained *C. elegans* on Bacto agar plates under standard conditions at 20°C.[32] We also cultivated animals at 15°C for testing the target cooling temperature. We utilized seven strains in our study: a wild-type N2 strain, a fluorescent strain with *daf-11(sa195)V*; *ofIs1[ptrx-1::trx-1::gfp]* for ASJ neuron imaging, CHB4526 *hmnEx2428[pIM48(pegl-13::gfp) + pRF4(rol-6(su1006))]* for embryo BAG and URX neuron imaging, fluorescent strains with *tax-2(p691)I*; *ofIs1* and *tax-2(p691)I*; *crh-1(tz2)III*; *ofIs1* for fluorescence measurements and ectopic outgrowth, and fluorescent strains with *dlk-1(ju476)I*; *vzEx29[p285(pssu-1::gfp) + pRF4]* and *dlk-1(ju476)I*; *crh-1(tz2)III*; *vzEx29* for ASJ regeneration frequencies. We utilized N2 for all experiments except for fluorescence imaging, where we utilized the strains with green fluorescent protein (GFP). We synchronized large populations of animals for experiments by placing ~30 adults on plates to lay eggs for 4 h. We transferred animals between plates using a pick. For the touch stimulus experiment, we used a pick to move animals at least 1 cm away from and then back to their original location.

METHOD DETAILS

Device design, components and assembling

We utilized Solidworks to design the stage and model its thermal distribution. Our design goal was an even and constant distribution. Components: Peltier heat pump (CP854705-2, 40 × 40 mm, from CUI Devices, Lake Oswego in Oregon); 99.9% pure copper stage block (100 × 140 × 3 mm, machined); sapphire window (80 mm diameter, 3 mm thickness, from Altos Photonics, Bozeman in Montana); Thermal paste to connect parts (Arctic MX-4, from Florence in South Carolina); water cooling pump tank for cooling water circulating (SC-300T, from Yosoo); copper liquid cooling heatsink (40 × 40 × 10 mm, unbranded); water cooling radiator to dispense all heat (12 Pipe, 240 mm with double fans, from DIYhz); silicone tubing for water flow (Nalgene™ 50, from Thermo Fisher Scientific, Waltham in Massachusetts); custom installation bracket fabricated by FDM (Fused Deposition Modeling) 3D printing of polylactide filament. Assembly and testing of the cooling stage follows procedures listed on a GitHub page (github.com/wormneurolab/CoolingStage/discussions). In brief, we first fix the sapphire window with wide packing tape (not pictured in Figure 1C) to the hole of the machined copper stage using thermal paste to fill gaps. Second, we place the cold surface of the Peltier on the matching location of the copper stage with thermal paste. Third, we place the heatsink on the hot surface of the Peltier with thermal paste and fix the assembly with the 3D printed installation bracket held by two screws. Fourth, we use silicone tubing to connect the heatsink, water pump tank, and water cooling radiator. Powering up the radiator and pump tank circulates water and removes heat pumped away from the cultivation plate by the Peltier heat pump.

Plate temperature measurements

We measured the thermal distribution of the agar plate using a calibrated thermal camera (Teledyne FLIR C2, Thousand Oaks in California). We embedded a wire digital thermocouple (Proster, San Jose in California) 1 mm into the agarose on plates to confirm camera readings and track agarose temperature over time.

Cooling methods: slow, fast, and abrupt

In general, the parameters of the cooling methods, such as voltages and times, that lead to the desired performance, will depend on specific parameters of the cultivation plates and stage, such as the amount of agar used to make the plates, the efficiency of the Peltier stage, and the material conductivities.

Slow cooling

In our study, we performed slow cooling on 20°C cultivated worm to a target temperature (T_{set}) of 6°C only. We first moved a cultivation plate with its lid to a 4°C refrigerator for 1 h. Then, we moved the plate directly to the cooling stage (pre-cooled for 10 min with 4.8 V across the Peltier), with the plate's lid off for better imaging and worm manipulation.

Fast cooling

We first moved a cultivation plate with animals to the cooling stage (cooled for 10 min at 12 V), with the plate lid removed. When the plate temperature reached T_{set} + 5°C, we turned the voltage to a lower value (4.8 V for T_{set} = 6°C and 7.1 V for T_{set} = 1°C) to avoid over-cooling and maintain plates at T_{set}. This method cools down plates to different target temperatures in ~15 min.

Abrupt cooling

In our study, we performed abrupt cooling to 6°C only. We moved individual animals from their cultivation plates directly to a pre-cooled 6°C plate resting on the cooling stage.

Tip-tracking

We first captured videos of animals under the stated conditions at 20 frames per second (FPS). Then, we extracted 1 frame per second from those videos using a custom MATLAB script. We manually tracked the nose tip position in those frames using the Multi-point Tool in ImageJ[31] and calculated velocities for each second in MATLAB. We averaged the individual velocities of 60 s to produce average velocities for each minute.

Lifespan and fecundity analysis

We collected N2 wild-type animals in the L4 lifestage on two plates. We left the control plate in the cultivation incubator. The cooled plate was processed by the slow cooling to 6°C and fast cooling to 1°C methods described above. We held animals at T_{set} for 1 h. We then moved the cooled plate back to the cultivation incubator.

Lifespan

A few hours after cooling or control treatment, we transferred animals to separate plates to avoid crowding. We observed animals twice daily following established procedure[33] to assess mortality. We transferred animals to new plates when needed to avoid starvation.

Fecundity

A few hours after cooling or control treatment, we transferred animals individually (*i.e.*, "singled") to plates. Three days later, we moved the singled animals to new plates and counted the number of hatched offspring for each animal. We repeated this process until there were no new offspring.

Fluorescence imaging

We used a Leica M205 FA widefield fluorescence stereomicroscope with 5×, 0.5 numerical aperture (NA) objective, and an Andor Zyla 4.2 sCMOS camera (Oxford Instrument; Concord, MA) to obtain images. We imaged neuronal GFP at 64× magnification, with theoretical 0.5 μm transverse and 4 μm axial resolution. We immobilized animals by slow cooling to 6°C. We performed single-frame, timelapse, and z-stack fluorescence imaging on the ASJ neuron with 100-ms exposure time. For timelapse imaging, we used 1 FPS for 2 min to obtain 120 frames in total. For z-stack imaging, we used a 3-axis stage (Thorlabs MBT616D, Newton in New Jersey) to obtain slices over a 40-μm z range, with 1-μm z step, and 4-s time interval between slices. For embryo imaging on the BAG and URX neurons we used 1 FPS with 200-ms exposure time.

Measurement of time expenditure for azide and cooling immobilization

To compare the efficiency of sodium azide and cooling immobilization, we recorded time spent on the processes needed to acquire a 2D image of the ASJ neuron in each of 100 animals (Table 1). We immobilized, manually located, imaged, and recovered animals in 4 batches, which reduces the length of time the animals are immobilized and improves animal viability. For comparison, we categorized processes into three general procedures: preprocessing, imaging, and postprocessing.

We performed sodium azide immobilization on 2% buffered agar pads with 5 mM azide following established procedure.[22] The preprocessing steps include making the agar-azide solution, fabricating and cooling agar pads, and mounting and arranging the animals on the agar pad. The postprocessing steps include recovering animals in buffer to rapidly remove azide, transferring recovered animals to cultivation plates, and moving cultivation plates back to the incubator. We believe the times we recorded accurately

represent user time expended in a typical high-resolution imaging experiment with azide immobilization. The time would increase if animals are sorted into groups (*e.g.*, surgery vs. mock), and the time would decrease if animal recovery is not required or if the agar-azide solution is reused.

We performed slow cooling immobilization to 6°C as described above. To optimize comparison with azide immobilization, we seeded with OP50 bacteria an area equal in size to our agar pads. Animals were largely confined to this area. We envision our cooling immobilization will be utilized on entire populations directly on their primary cultivation plates, so no transfer of animals is required. The preprocessing steps includes transferring plates to refrigerator and turning on the cooling stage. The postprocessing steps includes transferring plates to incubator.

Fluorescence, ectopic outgrowth, and regeneration measurements

We synchronized animals and imaged plates of young adults by slow cooling animals to 6°C. We obtained images at 2× magnification using our Leica M205 FA fluorescence microscope with an Andor Zyla 4.2 camera. For each ASJ cell body, we measured the brightest pixel value and subtracted the average pixel value for a nearby region (background). We followed our established protocol to measure frequency of ectopic outgrowth and regeneration.[23]

QUANTIFICATION AND STATISTICAL ANALYSIS

For comparing nose tip velocities, we calculated p-values using the t test: For different temperature settings or different cooling rates, we utilized the paired, two-tailed t test. For examining touch stimulus, we utilized the unequal variance, two-tailed t test.

For assessing differences in fluorescence, we calculated p-value by the unpaired, equal variance, two tailed t test. For determining differences in frequency of ectopic outgrowth and regeneration, we calculated p-value by Fisher's exact test.

For assessing the impact of cooling on viability and fecundity, we calculated p-value by using log-rank test and the unpaired, equal variance, two tailed t test, respectively. Data are represented as average ± standard deviation (SD). In figures, we indicate values that differ significantly at $p < 0.05$ (*) and $p < 0.001$ (**) levels.